Heliyon 10 (2024) e36664

Contents lists available at ScienceDirect

Heliyon

journal homepage: www.cell.com/heliyon

Research article

Transcriptome and proteomic analysis reveal the protective mechanism of acupuncture on reproductive function in mice with asthenospermia

Jianheng Hao [a,b], Jia Ren [b], Boya Chang [b], Huichao Xu [b], Haijun Wang [b,**], Laixi Ji [a,b,*]

[a] College of Acupuncture and Massage, Chengdu University of Traditional Chinese Medicine, Chengdu, 610075, China
[b] The Second Clinical College, Shanxi University of Traditional Chinese Medicine, Jinzhong, 030619, China

ARTICLE INFO

Keywords:
Transcriptomics
Proteomics
Acupuncture
Asthenozoospermia
Oxidative stress
Ferroptosis

ABSTRACT

Acupuncture is an integral component of complementary and alternative medicine that has been reported to enhance sperm motility, improve semen quality, and consequently augment male fertility. However, the precise mechanisms of action and the underlying molecular pathways remain unclear. In the present study, we aimed to elucidate the potential mechanisms through which acupuncture improves reproductive function in a mouse model of cyclophosphamide-induced asthenozoospermia. We collected sperm from the epididymis for semen analysis, collected serum to determine gonadotropin and oxidative stress marker levels, conducted histological examination of testicular tissue using hematoxylin and eosin (HE) and terminal deoxynucleotidyl transferase dUTP nick end labeling (TUNEL) staining, and observed mitochondrial morphology using transmission electron microscopy (TEM). We also assessed oxidative stress levels and total iron content in testicular tissue and validated the proteomic and transcriptomic analysis results of testicular tissue using real-time reverse transcription-quantitative polymerase chain reaction (RT-qPCR), protein imprinting analysis, and immunohistochemistry (IHC). Our results indicate that acupuncture enhances sperm quality in asthenozoospermic mice; increases serum testosterone (T), follicle-stimulating hormone (FSH), and luteinizing hormone (LH) levels; and attenuates oxidative damage, iron accumulation, and mitochondrial injury in mouse testicular tissues. Through protein and transcriptomic analyses, we identified 21 key genes, of which cytochrome *b*-245 heavy chain (CYBB), glutathione peroxidase 4 (GPX4), acyl-CoA synthetase long-chain family member 1 (ACSL1), and ferritin mitochondria (FTMT) were closely associated with ferroptosis. RT-qPCR, protein imprinting, and immunofluorescence (IF) analyses collectively indicated that acupuncture reduced ACSL1 and CYBB expression, and increased GPX4 and FTMT expression. Overall, the ferroptosis pathway associated with ACSL1/CYBB/FTMT/GPX4 represents a potential strategy through which acupuncture can improve the reproductive function in asthenozoospermic mice.

* Corresponding author. College of Acupuncture and Massage, Chengdu University of Traditional Chinese Medicine, Chengdu, 610075, China.
** Corresponding author.
E-mail address: jlx@sxtcm.edu.cn (L. Ji).

https://doi.org/10.1016/j.heliyon.2024.e36664
Received 9 May 2024; Received in revised form 20 August 2024; Accepted 20 August 2024
Available online 22 August 2024

1. Introduction

Infertility is the third most prevalent disease globally, after cancer and cardiovascular diseases. Epidemiological studies indicate that approximately 50 % of infertility cases are attributable to male factors [1]. Sperm vitality is a prerequisite for normal fertilization, as it enables sperm migration from the vagina to the fallopian tubes, egg penetration, and subsequent fusion with oocytes. Reduced sperm vitality, termed asthenozoospermia, is one of the most common causes of male infertility, and is characterized by either a below-threshold percentage of forward sperm motility (<32 %) or total sperm motility (<40 %) [2]. The etiology of this condition remains unclear, with potential associations with factors such as autoimmunity, infections, and genetics [3,4]. In addition to lifestyle modifications such as smoking cessation and alcohol reduction, pharmacological interventions such as gonadotropins, corticosteroids, or antioxidants constitute the primary treatment strategies for this condition [3,5]. However, the efficacy of these treatments is limited, often prompting patients to seek complementary and alternative approaches for improving pregnancy rates.

Acupuncture is an essential component of complementary and alternative medicine and a prevalent non-pharmacological treatment method. By stimulating specific acupoints, acupuncture has the potential to adjust the body's endocrine balance and improve the function of the reproductive system [6]. Several clinical trial studies [7–12] have indicated that patients with reduced fertility potential due to decreased sperm activity may benefit from acupuncture. Acupuncture may help improve sperm quantity, density, vitality, and morphology, thereby enhancing conception rates by promoting local blood circulation, ameliorating oxidative stress damage, and modulating hormone levels. In addition, multiple animal experiments have suggested that acupuncture may enhance sperm vitality by modulating hormone levels and testicular blood flow [13], increasing superoxide dismutase (SOD) activity levels to eliminate excess oxygen free radicals in the body [14], promoting the release of β-endorphins [15], and enhancing sperm acrosome reaction. The acupuncture technique known as "Zhibian (BL 54)-to-Shuidao (ST 28)" originated from the Inner Canon (Neijing) and was subsequently standardized and developed by Professor laixi Ji. It has been used to treat various reproductive system disorders in both men and women [16–18]. "Zhibian (BL 54)" refers to the acupuncture point located on the Bladder Meridian of the Foot Taiyang, which has the function of promoting the flow of meridians, clearing and benefiting the bladder. "Shuidao (ST 28)" refers to the acupuncture point on the Stomach Meridian of the Foot Yangming, which regulates water pathways, harmonizes menstruation, and benefits the kidneys. When acupuncture from "Zhibian (BL 54)" to "Shuidao (ST 28)" in an oblique direction, it stimulates the pelvic plexus nerves and perineal nerves, allowing the sensation of the needle to radiate to the surrounding genital area. This promotes the flow of "qi" to the affected area, thereby exerting a regulatory effect on nearby reproductive organs. In addition, based on traditional Chinese medicine (TCM), the bladder and kidney meridians are considered to have exterior-interior relationships. Acupuncture at this location simultaneously nourishes the kidneys and replenishes their essence, thereby enhancing the vitality of the reproductive system. Our preliminary experiments demonstrated that this acupuncture technique improved reproductive function in mice with asthenospermia. However, the exact therapeutic mechanisms underlying this technique are not fully understood.

Transcriptomics focuses on the sum of all the RNA produced during transcription in cells or tissue [19]. Transcriptomic analysis can help us understand the differences in mRNA levels before and after acupuncture treatment, identify regulated genes, and understand the effects of treatment on gene regulatory networks, which provide a basis for revealing the mechanism of acupuncture at the gene level and also provide clues for identifying novel therapeutic targets. Proteomics focuses on the overall expression and function of proteins in cells and tissues under specific conditions [20]. Through proteomic analysis, we can understand the composition and changes in proteins before and after acupuncture treatment to identify treatment biomarkers, providing reliable molecular standards for monitoring and evaluating treatment effects. By understanding the regulation of the protein interaction network and the effects of acupuncture on protein structure and modification, the molecular details of acupuncture treatment mechanisms can be further analyzed. Therefore, proteomics and transcriptomics have profound significance in the study of acupuncture treatment for asthenospermia. By combining the research in these two fields, we can understand the molecular basis and biological effects of acupuncture treatment of asthenospermia more comprehensively and provide a scientific basis for the optimization and refinement of acupuncture therapy.

In this study, we utilized a combined proteomics and transcriptomics approach to reveal the dynamic changes in biomolecules during acupuncture treatment. In addition, we validated selected key targets and signaling pathways to provide a deeper understanding of the molecular regulatory mechanisms underlying acupuncture therapy for asthenozoospermia.

2. Materials and methods

2.1. Experimental animal

Sixty male specific pathogen free (SPF) C57BL/6 mice aged 6–7 weeks were purchased from Sibeifu Animal Company (SCXK (JING)-2019-0010, Beijing, China). The mice weighed 18 ± 1 g and were housed at the Animal Experimental Center of Shanxi University of TCM. They were maintained under the following conditions: temperature of 25 ± 2 °C, humidity of 55 ± 5 %, with a 12-h light-dark cycle. The mice had ad libitum access to water and food and were allowed to acclimatize for 1 week prior to experimentation. All experimental procedures involving animals were performed in accordance with the National Institute of Health guidelines and approved by the Experimental Animal Ethics Committee of Shanxi University of TCM (approval no. AWE202303381).

2.2. Grouping and modeling

After 1 week of adaptation feeding, the mice were randomly divided into three groups: control, model, and acupuncture (ACU)

groups, with 20 mice in each group, using a random number table. Each morning, male mice in the model and acupuncture groups were intraperitoneally injected with cyclophosphamide (HY-17420, MedChemExpress, New Jersey, USA) at a dose of 50 mg/(kg·d) to induce asthenozoospermia [21]. The injection volume was 10 ml/kg. The control group was injected with an equal volume of 0.9 % NaCl solution for 5 d. Starting on the 6th day, each afternoon, the mice in the ACU group were placed in a prone position and fixed. The selected acupoints were locally disinfected with 75 % alcohol, followed by the use of disposable acupuncture needles (0.25 × 13 mm, Huatuo Medical Equipment Co., Ltd., Suzhou, China) to puncture the bilateral "Zhibian (BL 54)" points (at the lateral side of the mouse's buttocks, at the point where the line connecting the greater trochanter of the femur and the midpoint of the fourth sacral bone meets the bony fissure) diagonally toward the ipsilateral "Shuidao (ST 28)" points (approximately 8 mm below the upper 2/3 and the lower 1/3 junction of the xiphoid process to the pubic symphysis, approximately 3 mm beside the midline) [22]. The depth of needle insertion was approximately 5 mm, and each session lasted for 20 min, once daily for consecutive 2 weeks. The control and model groups underwent fixation without any intervention. On the day after the completion of treatment, the mice from each group were anesthetized with isoflurane gas, and various samples were collected based on the experimental requirements for subsequent experiments.

2.3. Determination of testicle, epididymis mass and index

Testicular and epididymal tissues were aseptically harvested from both sides of the mice, excess fat tissue was removed, the tissues were placed on filter paper to remove excess moisture, and the testicles and epididymides were weighed using an electronic balance. The corresponding organ indices were calculated using the following formula: Organ Index (either testicular or epididymal) = (weight of the respective organ/body weight measured immediately before euthanasia) × 100 %.

2.4. Epididymal sperm analysis

The epididymides were placed in culture dishes. A suitable amount of 0.9 % sodium chloride solution was added. Using a disposable sterile syringe needle, the tissue was gently punctured to release the sperm into a 0.9 % sodium chloride solution. After incubating at 37 °C for 15 min to ensure the sperm were thoroughly dispersed, the suspension was pipetted onto a sperm counting plate. Computer-assisted sperm analysis (CASA) was performed using a system (WLJY-9000; Weili Corporation, China).

2.5. Determination of testosterone (T), follicle-stimulating hormone (FSH) and luteinizing hormone (LH) in serum

Based on the instructions for the T-assay kit (MU30398, Bio-swamp, Wuhan, China), FSH assay kit (MU30265, Bio-swamp), and LH assay kit (MU30382, Bio-swamp), standards, serum samples, and sample diluents were sequentially added to a 96-well plate. The plate was sealed, incubated, washed, and subjected to color development. Finally, using an enzyme immunoassay reader (Spectra Max Plus384, Molecular Devices, Sunnyvale, CA, USA), the absorbance values at 450 nm for each experimental well were observed and recorded. The corresponding concentrations of T, FSH, and LH were calculated using standard curves.

2.6. Hematoxylin and eosin (HE) staining

Testicular and epididymal tissues were fixed for 48 h, followed by routine dehydration, clearing, embedding in paraffin, and preparation into 5 μm paraffin sections (RM2145, Leica, Wetzlar, Germany). Subsequently, the sections were deparaffinized in water and stained with hematoxylin and eosin for 3 min. The sections were then dehydrated using a gradient of 85 % and 95 % ethanol, followed by staining with eosin for 5 min. After dehydration, the sections were mounted with a coverslip and pathological changes in the testicular and epididymal tissues of each group were observed under a microscope (ECLIPSE Ci-S, Nikon, Tokyo, Japan).

2.7. Terminal deoxynucleotidyl transferase dUTP nick end labeling (TUNEL) staining

Paraffin-embedded testicular tissue sections were deparaffinized in water and washed with phosphate-buffered saline (PBS). Then, 100 μL of proteinase K from the TUNEL assay kit (G1504, Servicebio, Wuhan, China) was added and incubated at 37 °C for 20 min, followed by washing thrice with PBS for 5 min each time. Subsequently, membrane permeabilization solution was added and incubated at 37 °C for 20 min, followed washing thrice with PBS for 5 min. Thereafter, 50 μL of equilibration buffer was added and incubated at room temperature for 10 min. Next, reaction solution was added to cover the tissue and incubated in a humid chamber at 37 °C for 1 h, followed by washing thrice with PBS for 5 min each time. Next, 4',6-diamidino-2-phenylindole (DAPI) staining solution was added and incubated at room temperature in the dark for 10 min, followed by washing thrice with PBS for 5 min each time. After mounting, sections were observed and photographed using a fluorescence microscope (DM750; Leica, Wetzlar, Germany).

2.8. Real-time reverse transcription-quantitative polymerase chain reaction (RT-qPCR) analysis

Total RNA was extracted from testicular tissues (G3013; Servicebio, Wuhan, China). The extracted total RNA was reverse-transcribed into complementary deoxyribonucleic acid (cDNA) (G3337, Servicebio, Wuhan, China). The resulting cDNA from the reverse transcription was used as a template for PCR amplification (with the following conditions: 95 °C for 30 s, 1 cycle; 95 °C for 15 s, 60 °C for 30 s, 40 cycles). After the reaction, the Ct values of each well were determined using a PCR detection system (CFX 96; Bio-

Rad, Hercules, California, USA). The results were normalized to GAPDH and the relative mRNA expression levels of the target gene were calculated using the $2^{-\Delta\Delta CT}$ formula. Primers used for qRT-PCR are listed in Table 1.

2.9. Western blot analysis

Total protein was extracted from the mouse testicular tissues. Protein concentration was determined using the bicinchoninic acid (BCA) method (G2026, Servicebio, Wuhan, China). Each well was loaded with 10 μL of protein sample after gel preparation, and electrophoresis was performed. Following wet transfer for 2 h, the membranes were blocked with 5 % nonfat milk for 2 h. After washing, membranes were probed with primary antibodies against b-cell lymphoma-2 (BCL-2) (GB124830, Servicebio, Wuhan, China), bcl-2 associated x protein (BAX) (GB12690, Servicebio, Wuhan, China), caspase-3 (GB11767C, Servicebio, Wuhan, China), cytochrome *b*-245 heavy chain (CYBB) (GB112362, Servicebio, Wuhan, China), glutathione peroxidase 4 (GPX4) (GB124327, Servicebio, Wuhan, China), acyl-coA synthetase long chain family member 1 (ACSL1) (A22737, Abclonal, Wuhan, China), and ferritin mitochondrial (FTMT) (PA5-30906, Thermofisher, Massachusetts, USA) overnight at 4 °C (all antibodies were diluted 1:1000 except β-actin, which was diluted 1:3000). The following day, the membranes were washed with Tris-buffered saline containing Tween 20 (TBST) and incubated with secondary antibodies (GB23303; Servicebio, Wuhan, China) at room temperature for 1 h (diluted 1:5000). After washing, the membranes were incubated with developing solution and visualized using a gel imaging system (HOOD-II; Bio-Rad, Hercules, California, USA). Images were captured and saved. Finally, the gray values of the bands were measured using ImageJ software (Bethesda, Maryland, USA), and the relative expression levels of target proteins were compared between groups using the ratio of the gray values of target proteins to those of internal reference proteins.

2.10. Protein sequencing and analysis

Four testicular tissue samples were selected randomly from each group. Initially, efficient protein extraction and quantification were performed using sodium dodecyl sulfate, dithiothreitol, and Triton X-100 (SDT) buffer, and a bicinchoninic acid (BCA) protein assay kit (5000001, Bio-Rad, California, USA). Subsequently, protein digestion was performed using a filter-aided sample preparation (FASP) method, which involves multiple ultrafiltration and washing steps to effectively remove low-molecular-weight impurities. The resulting peptides were desalted using an octadecyl (C18) column (66872; Sigma, St. Louis, Missouri, USA). During sodium dodecyl sulfate-polyacrylamide gel electrophoresis (SDS-PAGE) protein electrophoresis stage, proteins were separated on a 12.5 % SDS-PAGE gel after boiling with loading buffer, and protein bands were visualized by Coomassie Blue R-250 staining. Tandem mass tag (TMT) reagents (90064CH; Thermo Fisher Scientific, Waltham, Massachusetts, USA) were used to label the peptide mixtures from each sample. Subsequently, the labeled peptides were analyzed using high-pH reverse-phase separation and liquid chromatography-tandem mass spectrometry (LC-MS/MS). Peptide separation was achieved using a Q Exactive mass spectrometer (Orbitrap Exploris 120, Thermo Fisher Scientific, Massachusetts, USA) coupled with an Easy nLC (Vanquish, Thermo Fisher Scientific, Massachusetts, USA) to generate high-quality mass spectrometry data. Finally, protein identification and quantification were performed using the matrix science automated search for peptide identification from the tandem mass spectra (MASCOT) engine embedded in Proteome Discoverer 1.4 software.

In the bioinformatics analysis stage, we first screened for significantly differentially expressed proteins (DEPs) based on fold change (FC) $>$ 1.2-fold (upregulation of $>$1.2-fold or downregulation of $<$0.83-fold) and $P < 0.05$ (T-test as the standard. To analyze the expression patterns both between and within sample groups, and to assess the rationality of the grouping in our project, we used Cluster 3.0 (http://bonsai.hgc.jp/~mdehoon/software/cluster/software.htm) and Java TreeView (http://jtreeview.sourceforge.net) to conduct hierarchical clustering analyses. CELLO (http://cello.life.nctu.edu.tw/), a multiclass SVM classification system, was used to predict subcellular protein localization. Protein sequences were searched using InterProScan software to identify protein domain

Table 1
Primer sequences.

Gene	Primer sequences (5′–3′)	Amplicon size (bp)
BAX	Forward: TTGCTACAGGGTTTCATCCAGG Reverse: GCAAAGTAGAAGAGGGCAACCA	275
Caspase-3	Forward:TGGAATGTCATCTCGCTCTGGT Reverse: GAAGAGTTTCGGCTTTCCAGTC	298
BCL-2	Forward:TGACTTCTCTCGTCGCTACCGT Reverse: CCTGAAGAGTTCCTCCACCACC	112
GPX4	Forward: GAGGCAGGAGCCAGGAAGTAA Reverse: CACCACGCAGCCGTTCTTAT	214
ACSL1	Forward: TGCCACAGTGCTGACGTTTC Reverse: CCCTTGGATGCCAGGTAATT	195
FTMT	Forward: CTATCAACCGCCAAATCAACCT Reverse: CGCATTCCCAGTCATCTTTATCT	231
CYBB	Forward:GTTCCAGTGCGTGTTGCTCG Reverse: TCCCGACTCTGGCATTCACA	156
GAPDH	Forward: CCTCGTCCCGTAGACAAAATG Reverse: TGAGGTCAATGAAGGGGTCGT	133

signatures from the InterPro member database Pfam. For Gene Ontology (GO) annotation, differentially expressed protein sequences were locally searched using the Basic Local Alignment Search Tool (BLAST) + client software and InterProScan to identify homologous sequences. These sequences were annotated with GO terms using Blast2GO, and the results were plotted using R scripts. Kyoto Encyclopedia of Genes and Genomes (KEGG) annotation involved blasting the studied proteins against the KEGG database (http://geneontology.org/) to retrieve KEGG orthology identifications and map them to KEGG pathways. Enrichment analysis was conducted using Fisher's exact test using the entire set of quantified proteins as the background dataset. To adjust for multiple testing, the Benjamini-Hochberg correction was applied, considering only functional categories and pathways with $P < 0.05$.

2.11. Transcriptome sequencing and analysis

Total RNA was extracted from four randomly selected testicular tissue samples from each group. The concentration and purity of the samples were determined using a NanoDrop spectrophotometer (NC2000; Thermo Fisher Scientific, Waltham, MA, USA). RNA integrity was assessed using an Agilent 2100 Bioanalyzer (Agilent 2100, Agilent Technologies, California, USA). Poly(A)-tailed mRNA were enriched using oligo (dT) magnetic beads. The mRNA was fragmented into smaller pieces using divalent cations at elevated temperatures. These fragments served as templates for cDNA synthesis and were primed with random oligonucleotides. The resulting double-stranded cDNA was purified, end-repaired, and a single 'A' base was added to the 3′ ends, followed by the ligation of sequencing adapters. cDNA fragments of approximately 400–500 bp were selected using AMPure XP beads (A63880; Beckman Coulter, California, USA), amplified by PCR, and purified again using AMPure XP beads to obtain the final library. Sequencing was performed using an Illumina sequencer (HiSeq, Illumina, California, USA) with assistance from Shanghai Personal Biotechnology Co., Ltd., China.

After sequencing, raw data were generated and filtered to remove reads containing adapters and low-quality reads, ensuring that all subsequent analyses were based on clean, high-quality data. The reference genome and annotation files were downloaded from the genome website (reference genome: GCF_000001635.27_GRCm39_genomic.fna). Clean paired-end reads were aligned to the reference genome using HISAT2 (v2.1.0). HTSeq (version 0.9.1) was used to count the number of reads mapped to each gene, which served as the raw expression level. Expression levels were normalized to fragments per kilobase per million (FPKM). Differentially expressed genes (DEGs) between the two groups were identified using DESeq (1.20.0) with a threshold of $|\log2FC| > 1$ and significance $P < 0.05$. Venn diagrams were plotted to identify the key DEGs. GO functional enrichment analysis of key DEGs was performed using topGO software (v2.50.0) to determine the primary biological functions of the differentially expressed genes. KEGG pathway enrichment analysis was conducted using ClusterProfiler (v4.6.0), focusing on pathways with $P < 0.05$.

2.12. Determination of SOD activity and GSH, malondialdehyde (MDA), and Fe content in testicular tissue and serum

Testicular tissue was homogenized in 0.9 % saline solution under ice-cold conditions to prepare a 10 % homogenate, followed by centrifugation at 4 °C, 2500–3000 rpm for 10 min. The supernatant was collected for further analysis. Whole blood samples were centrifuged at 4 °C, 3000 rpm for 15 min after standing at room temperature for 2 h, and the supernatant was collected for testing. Based on the instructions of different assay kits, the total superoxide dismutase (T-SOD) activity (A001-1, Jiancheng, Nanjing, China) and reduced glutathione (GSH) (G4305, Servicebio, Wuhan, China), MDA (A003-1, Jiancheng, Nanjing, China), and total iron (GM1162, Servicebio, Wuhan, China) levels were determined separately in testicular tissue.

2.13. Transmission electron microscopy (TEM) analysis

Fresh testicular tissue samples smaller than 1 mm were washed with a buffer solution and fixed in a glutaraldehyde solution at room temperature for 2 h. After washing again, the samples were fixed with osmium tetroxide, dehydrated through a gradient, embedded in resin, sectioned, stained, and observed and images were captured using a TEM (HT7800, HITACHI, Tokyo, Japan).

2.14. Immunofluorescence (IF) and immunohistochemistry (IHC) analysis

Frozen sections of testicular tissue were incubated with a reactive oxygen species (ROS) staining solution (D7008, Sigma, Missouri, USA) for 30 min in the dark. Excess liquid on the tissue surface was removed and the cell nuclei were counterstained with DAPI and incubated in the dark for 10 min. The sections were sealed, and images were captured using a fluorescence microscope.

Testicular tissue paraffin sections were dewaxed in water and antigen retrieval (G1202, Servicebio, Wuhan, China) was performed, followed by blocking with 5 % bovine serum albumin (BSA) (GC305010, Servicebio, Wuhan, China) for 30 min. Primary antibodies (ACSL1 dilution ratio: 1:200, FTMT dilution ratio: 1:500, CYBB and GPX4 dilution ratio: 1:1000) were added and incubated overnight at 4 °C. After rewarming, secondary antibodies (GB21303; Servicebio, Wuhan, China) were added and incubated for 50 min at (dilution of 1:300). 3,3′-diaminobenzidine (DAB) (G1212, Servicebio, Wuhan, China) was then added for color development, followed by counterstaining with hematoxylin and sealing of the slides. Finally, Image-Pro Plus software (version 6.0; Media Cybernetics, Inc., Bethesda, MD, USA) was used to analyze the images.

2.15. Statistical analysis

All statistical analyses were conducted using the GraphPad Prism 8.01 software (La Jolla, CA, USA). Data are presented as mean ± standard deviation (SD). One-way analysis of variance (ANOVA) followed by a post hoc least significant difference (LSD) test was used

to calculate the statistical significance between groups, and $P < 0.05$ was considered to indicate statistical significance.

3. Results

3.1. Acupuncture improves the reproductive function of mice with asthenozoospermia

We analyzed the effects of acupuncture on the testis, epididymal coefficient, and sperm quality in mice (Fig. 1A and B). Compared to the control group, the model group showed significant decreases in testis weight, testis coefficient, epididymal weight, and epididymal coefficient ($P < 0.01$) as well as decreases in total sperm count, sperm vitality, and sperm motility ($P < 0.01$). Compared to the model group, the ACU group showed increases in testis and epididymal weight, testis coefficient ($P < 0.01$), total sperm count, sperm vitality, and sperm motility ($P < 0.01$); however, there was no difference in the epididymal coefficient ($P > 0.05$). Asthenozoospermia is often accompanied by disturbances in serum hormone levels, which reflect the functional status of the reproductive system. In the present study, we showed that compared to the control group, mice from the model group showed varying degrees of decrease in T, FSH, and LH serum levels ($P < 0.01$). In contrast, compared to the model group, mice from the ACU group showed varying degrees of increase in T, FSH, and LH serum levels ($P < 0.01$) (Fig. 1C).

We conducted a histopathological analysis of the testes and epididymis using HE staining (Fig. 1D and E). In the control group, the seminiferous tubules in the testicular tissue exhibited intact tubular walls, regular lumens, and clear and intact basement membranes, with abundant mature free spermatozoa visible in the central lumen. In the model group, the seminiferous tubules in the testicular tissue showed partial morphological abnormalities, a disordered arrangement, uneven tubular wall thickness, significantly reduced mature spermatozoa in the central lumen, and a decreased number of interstitial cells distributed between the seminiferous tubules with deteriorated cell morphology. In the control group, the epididymal tubules in epididymal tissue displayed intact structures, an orderly arrangement of epithelial cells, smooth lumens, and abundant spermatozoa. In the model group, some epididymal tubules exhibited morphological abnormalities, disordered layers, uneven tubular wall thickness, vacuolation, fewer mature spermatozoa in the lumen, and damage to the epididymal interstitium between the epididymal tubules. In the ACU group, testicular and epididymal histopathological morphology as well as the number of spermatozoa in the lumen improved to varying degrees.

3.2. Acupuncture improves testicular tissue cell apoptosis in asthenozoospermia mice

We assessed the effects of acupuncture on apoptosis in the testicular tissue and key apoptotic factors using TUNEL staining, RT-qPCR, and western blotting. In Fig. 2A, green fluorescence represents apoptotic cells primarily distributed near the basement membrane of the seminiferous tubules, especially around spermatogonia. Compared with the control group, the model group showed a significant increase in the rate of positive cell apoptosis in the testicular tissue ($P < 0.01$). Compared with the model group, the ACU group exhibited a significant decrease in the rate of positive cell apoptosis in the testicular tissue ($P < 0.01$) (Fig. 2A and B). The balance of regulation among Caspase-3, BCL-2, and BAX is an important factor in determining cell survival and apoptosis. Compared to the control group, the model group showed increased relative expression of BAX and Caspase-3 proteins and mRNA in testicular tissue ($P < 0.01$), whereas the relative expression of BCL-2 protein and mRNA decreased ($P < 0.01$). Compared to the model group, the ACU group of mice showed decreased relative expression of BAX and Caspase-3 proteins and mRNA in testicular tissue ($P < 0.01$), and increased relative expression of BCL-2 protein and mRNA ($P < 0.01$) (Fig. 2C and D) (Western blot original images are provided in Supplementary 3).

3.3. Proteomic analysis

A total of 8135 proteins were identified in all testicular tissue samples, of which 8123 were quantifiable and accounted for 99.85 % of the total protein count (Fig. 3A). To further analyze the experimental data, we performed differential screening of proteins with expression changes based on the criteria of FC > 1.2-fold (upregulated by more than 1.2-fold or downregulated by less than 0.83-fold) and P value < 0.05 (Supplementary 1). Compared to the control group, the model group showed 541 upregulated and 986 downregulated proteins. Compared to the model group, the ACU group exhibited 44 upregulated and 82 downregulated proteins. To illustrate the significant differences in protein expression between the control group vs. model group and the model group vs. ACU group, volcano plots were generated based on fold change and P-value (*t*-test) criteria (Fig. 3B and C). In addition, cluster analysis of differentially expressed proteins indicated (Fig. 3D and E) a high similarity in protein expression patterns within each group and a lower similarity in protein expression patterns among groups, demonstrating that the identified differentially expressed proteins were reasonable and accurate, meeting the conditions for further analysis.

Subcellular organelles are microstructures within the cytoplasm with specific shapes and functions that serve as important sites for proteins to perform their various functions. Different organelles often perform different cellular functions; therefore, analyzing the subcellular localization of proteins contributes to further understanding of the functions of proteins within the cell. We found that the differentially expressed proteins between the control group vs. the model group and the model group vs. the ACU group were primarily localized in the cell nucleus (Fig. 3F and G). We also predicted the structural domains of these differentially expressed proteins. The differentially expressed proteins between the control and model groups were primarily concentrated in domains such as the protein kinase domain and trypsin, whereas those between the model and ACU groups were primarily concentrated in domains such as the Immunoglobulin V-set domain and trypsin (Fig. 3H and I). This is important for studying the critical functional regions of proteins and their potential biological roles.

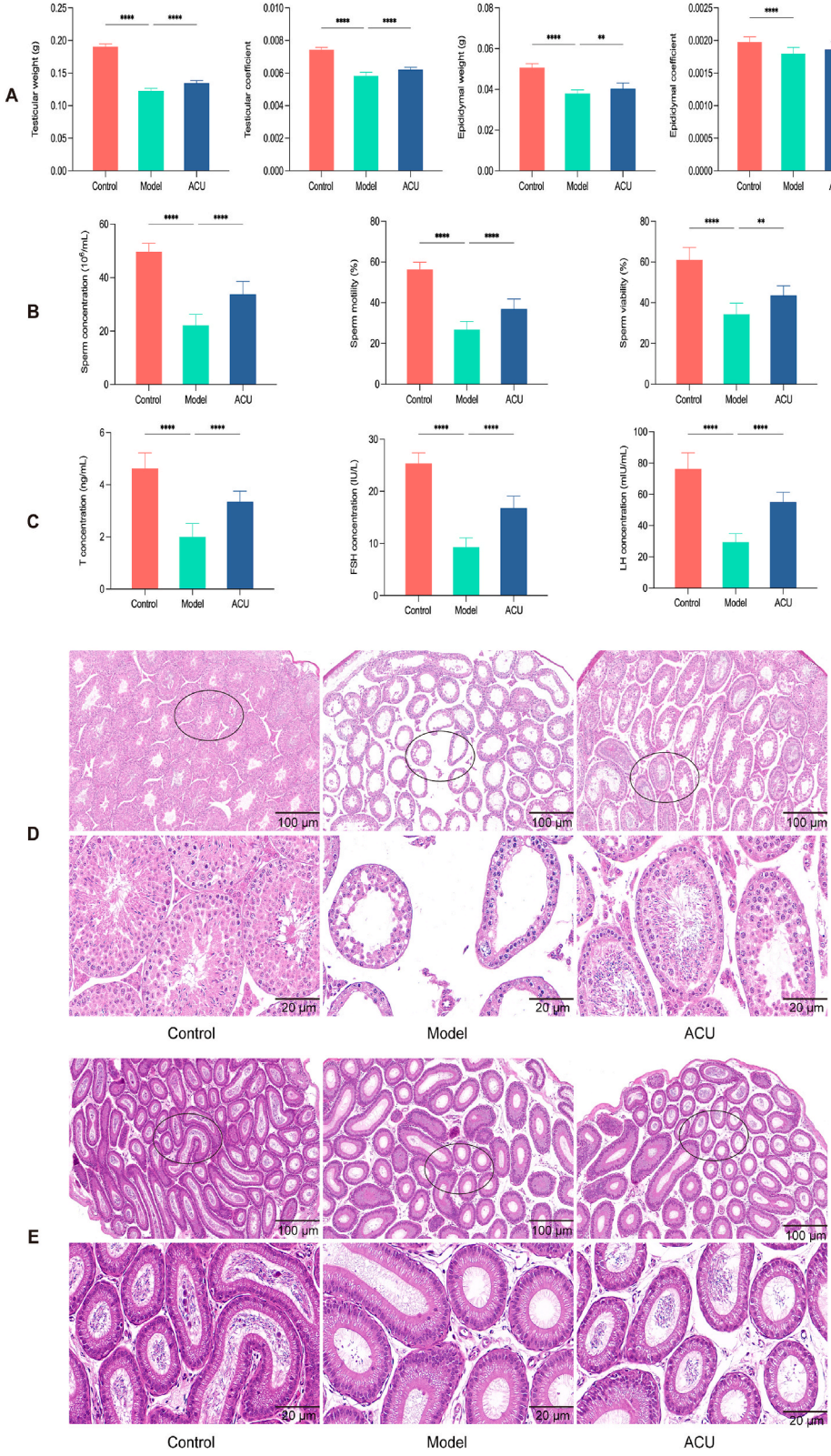

(caption on next page)

Fig. 1. Acupuncture improves reproductive function in asthenozoospermia mice. (A) Comparison of testis and epididymis coefficients among groups (n = 20). (B) Comparison of sperm quality among groups (n = 10). (C) Comparison of serum levels of T, FSH, and LH among groups (n = 10). (D) Comparison of testicular tissue pathological morphology among groups (× 100, × 400). (E) Comparison of epididymal tissue pathological morphology among groups (× 100, × 400). Data are presented as mean ± SD. *$P < 0.05$; **$P < 0.01$, ***$P < 0.001$, ****$P < 0.0001$.

This study investigated the mechanism of action of acupuncture on asthenozoospermia in mice. Therefore, we primarily focused on the commonly shared DEPs between the model and control groups, and the ACU and model groups (Fig. 3J). A total of 102 common DEPs were identified, of which 30 were upregulated in the model group and downregulated after acupuncture, whereas 25 were downregulated in the model group and upregulated after acupuncture. As these 55 DEPs showed significant differential expression before and after modeling and treatment, they may serve as potential target proteins for acupuncture to improve asthenozoospermia. To comprehensively understand the functions, localization, and biological pathways associated with these key DEPs, we conducted GO functional enrichment analysis (Fig. 3K). GO analysis revealed enrichment of 86 biological processes (BPs), seven cellular components (CCs), and 41 molecular functions (MFs). These DEPs primarily participate in processes such as fatty acid metabolism and lipid transport, occur primarily in cellular components such as peroxisomes and microbodies, and are closely related to functions such as antioxidant and peptidase regulator activities. To systematically decipher the potential mechanisms of acupuncture, we annotated and analyzed these key DEPs using KEGG pathways (Fig. 3L). KEGG analysis revealed the enrichment of 129 signaling pathways. These target points primarily involve signaling pathways, such as the peroxisome proliferator-activated receptor (PPAR) signaling pathway and ferroptosis, and are associated with cholesterol metabolism and fatty acid degradation.

3.4. Transcriptomic analysis

Principal component analysis of the transcriptome revealed significant differences between groups (Fig. 4A). Based on the criteria $|\log2FC| > 1$ and significance P-value <0.05, 4021 differentially expressed genes (DEGs) were identified (Supplementary 2). Among them, there were 2242 DEGs between the control and model groups (727 upregulated and 1715 downregulated), and 354 DEGs between the model and ACU groups (286 upregulated and 59 downregulated). To illustrate the significant differences in gene expression between the control group vs. the model group and the model group vs. the ACU group, volcano plots were generated based on the FC and P value (*t*-test) criteria (Fig. 4B and C). In addition, heatmap clustering showed distinct differences in the DEGs among the groups (Fig. 4D and E), thus meeting the criteria for further analysis.

We identified 268 common DEGs between the model group and the control group, and the ACU group vs. the model group as the primary focus of our study. The Venn diagram (Fig. 4F) shows that 40 DEGs were upregulated in the model group and downregulated after acupuncture treatment, whereas 227 DEGs were downregulated in the model group and upregulated after acupuncture treatment. Therefore, these 267 DEGs were considered as potential therapeutic targets for asthenozoospermia and were used for subsequent functional enrichment analysis. GO analysis revealed the enrichment of 2256 BPs, 195 CCs, and 373 MFs. These DEGs were primarily involved in processes such as spermatid development and differentiation, occurring primarily in cellular components such as acrosomal vesicles and nucleotide-activated protein kinase complexes, and were closely related to functions such as lysozyme and protein-disulfide reductase (NAD (P)) activities (Fig. 4G). KEGG analysis identified enrichment in 197 signaling pathways. These target genes were primarily associated with signaling pathways such as cerroptosis and the calcium signaling pathway, while also being related to processes such as arginine and proline metabolism and protein digestion and absorption (Fig. 4H).

3.5. Integrated transcriptomic and proteomic analysis

By identifying the intersection of DEGs and DEPs, we were able to more accurately identify genes that were commonly upregulated or downregulated to determine potential therapeutic targets. The Venn diagram (Fig. 5A) shows that eight genes were upregulated in the model group and downregulated after acupuncture treatment, whereas 13 genes were downregulated in the model group and upregulated after acupuncture treatment. We conducted functional enrichment analysis of these 21 commonly expressed genes. GO analysis revealed enrichment of 513 BPs, 38 CCs, and 87 MFs. The primary BP is involved in the fusion of sperm to the egg plasma membrane, which is involved in single fertilization, plasma membrane fusion, and response to oxidative stress. These genes primarily occur in cellular components such as acrosomal vesicles and collagen-containing extracellular matrix, and are closely related to functions such as antioxidant activity and growth factor binding (Fig. 5B). KEGG analysis identified enrichment of 57 signaling pathways. These target genes are primarily involved in signaling pathways such as ferroptosis and the advanced glycation end products-receptor for advanced glycation end products (AGE-RAGE) signaling pathway in diabetic complications, while also being related to processes such as protein digestion, absorption, and fatty acid biosynthesis (Fig. 5C). In addition, we visualized key pathway genes using a net plot (Fig. 5D). In conclusion, we speculate that ACSL1/CYBB/FTMT/GPX4 may be a critical target gene in the ferroptosis pathway that is improved by acupuncture in asthenozoospermic mice.

3.6. Acupuncture improves oxidative stress and iron metabolism in asthenozoospermia mice

Ferroptosis is a regulatory form of cell death that depends on iron and reactive oxygen species (ROS). When excessive iron accumulates within cells, lipid peroxidation occurs on the unsaturated fatty acids of the cell membrane due to the Fenton reaction, leading to increased ROS production and oxidative damage, ultimately inducing cell death [23]. Compared to the control group, mice

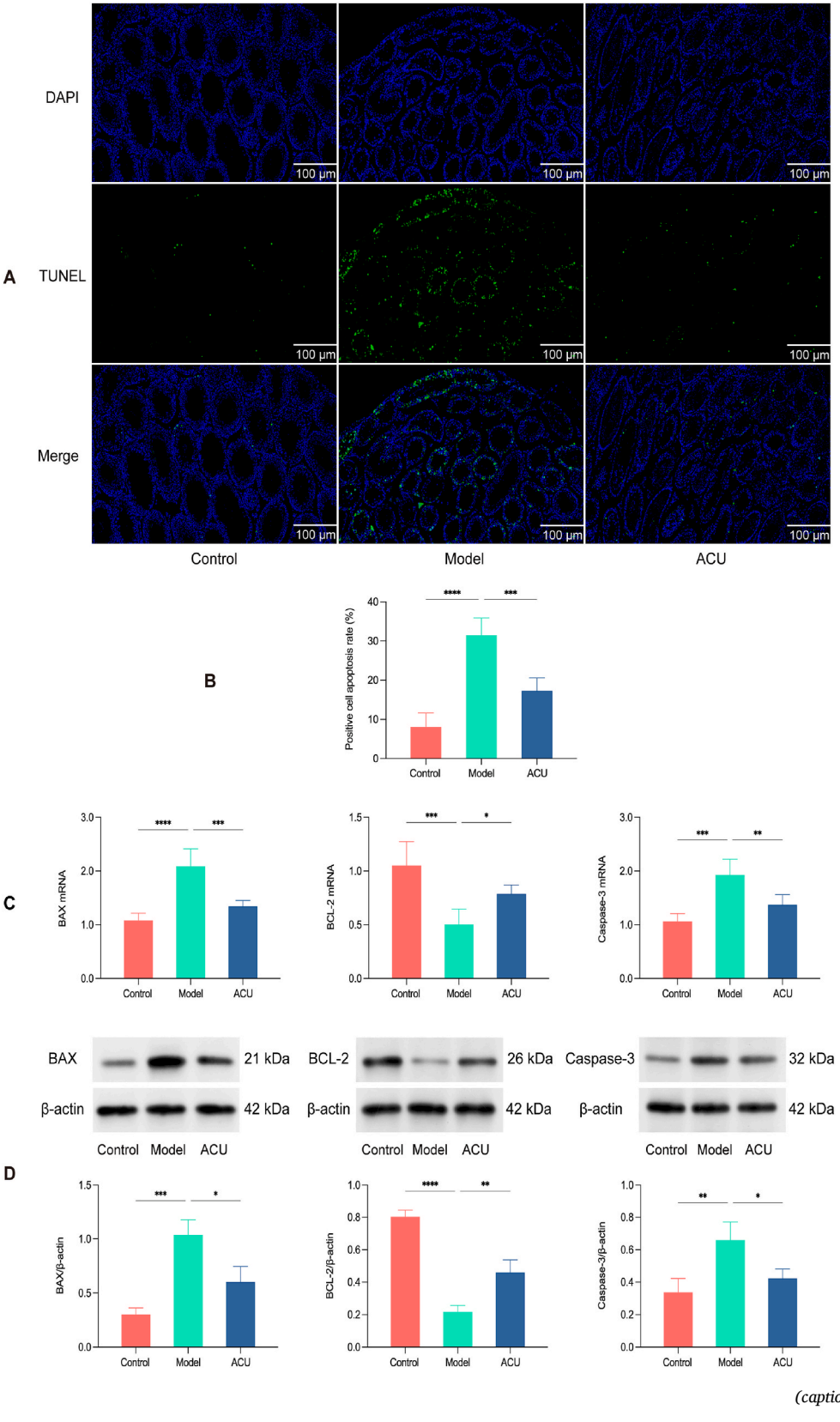

(caption on next page)

Fig. 2. Acupuncture improves apoptosis of testicular tissue. (A–B) Comparison of apoptotic rates of positive cells in testicular tissue among groups (TUNEL staining, × 200) (n = 5). (C) Comparison of relative expression levels of BCL-2, BAX, and Caspase-3 mRNA in testicular tissue of mice among groups (n = 5). (D) Comparison of relative expression levels of BCL-2, BAX, and Caspase-3 protein in testicular tissue of mice among groups (n = 3) (Western blot original images are provided in Supplementary 3). Data are presented as mean ± SD. *$P < 0.05$; **$P < 0.01$, ***$P < 0.001$, ****$P < 0.0001$.

in the model group showed a significant decrease in serum T-SOD activity and GSH levels ($P < 0.01$, $P < 0.05$, respectively), along with an increase in MDA levels ($P < 0.01$) (Fig. 6A). In the testicular tissue, T-SOD activity and GSH levels decreased to varying degrees ($P < 0.01$), whereas MDA, total iron, and ROS levels increased ($P < 0.01$) (Fig. 6B–D). Following acupuncture intervention, GSH levels increased ($P < 0.01$) and MDA levels decreased ($P < 0.01$) in the serum (Fig. 6A), whereas T-SOD activity and GSH levels in the testicular tissue increased to varying degrees ($P < 0.01$), and MDA, total iron, and ROS levels decreased to varying degrees ($P < 0.01$, $P < 0.05$) (Fig. 6B–D).

Mitochondria are crucial sites where oxidative stress triggers biological effects. To further ascertain the extent of oxidative damage in the testes, we used TEM to observe the ultrastructure of the testicular tissue (Fig. 6E). Compared to the control group, mice in the model group exhibited a decrease in the number of mitochondria in the testicular tissue, along with structural deformation, incomplete or swollen mitochondria, and ruptured or missing cristae accompanied by numerous vacuoles. Conversely, compared to the model group, mice in the ACU group showed an increase in the number of mitochondria in testicular tissue, along with varying degrees of improvement in the morphological structure.

3.7. Acupuncture improves testicular ferroptosis in asthenozoospermia mice by regulating ACSL1/CYBB/FTMT/GPX4

We validated the changes in the ferroptosis-related markers ACSL1/CYBB/FTMT/GPX4 at the protein and mRNA levels using RT-qPCR and western blotting. These trends were consistent with the results of proteomic and transcriptomic sequencing (Fig. 7A and B) (Western blot original images are provided in Supplementary 3). Compared to the control group, the relative expression of ACSL1 and CYBB proteins and mRNA in the testicular tissue of the model group were increased ($P < 0.01$, $P < 0.05$), whereas the expression of FTMT and GPX4 proteins and mRNA were decreased ($P < 0.01$). Compared to the model group, the relative expression of ACSL1 and CYBB proteins and mRNA in the testicular tissue of the ACU group were decreased ($P < 0.01$, $P < 0.05$), whereas the expression of GPX4 protein and mRNA were increased ($P < 0.01$, $P < 0.05$) and the expression level of FTMT mRNA was increased ($P < 0.05$). Finally, we performed IHC to determine ACSL1/CYBB/FTMT/GPX4 expression in testicular tissue and found that ACSL1/CYBB/FTMT/GPX4 was primarily expressed in spermatogenic and interstitial cells (Fig. 7C). Compared to the model group, the expression of GPX4 in the testicular tissue of the ACU group were increased ($P < 0.01$), whereas the expression of ACSL1 and CYBB were decreased ($P < 0.01$, $P < 0.05$) (Fig. 7D).

4. Discussion

Sperm, as a specialized cell, primarily relies on flagella for movement. Following ejaculation, the sperm enters the female vagina, successfully traverses the cervix through movement, binds to the egg in the fallopian tube, and completes fertilization. Therefore, a sufficient quantity of forward-moving sperm is essential for successful conception, and sperm vitality is a critical reference indicator of male fertility [24]. Cyclophosphamide is an alkylating agent primarily used in cancer therapy by disrupting the structure and function of deoxyribonucleic acid (DNA), leading to cellular damage [25]. However, this damaging effect can also affect other normal cells, particularly those in the reproductive system [26]. Clinical studies have found that cyclophosphamide treatment in male patients may increase the incidence of oligoasthenozoospermia and azoospermia, while also promoting testicular damage and disruption of gonadotropin secretion in the bloodstream [27,28]. Animal experiments have shown that cyclophosphamide can decrease sperm count, alter morphology and motility in mice, and cause damage to reproductive organs, such as the testes, resulting in decreased fertility and potential hereditary abnormalities in the offspring [29,30]. T, FSH, and LH play crucial roles in the regulation of testicular function and sperm production [31–34]. T, as the primary male hormone, promotes sperm formation and development, and maintains sperm quality and fertilization ability. FSH primarily stimulates the maturation of secondary spermatocytes and helps to maintain stable testosterone levels in the testes. LH stimulates Leydig cells to produce testosterone, thereby maintaining testosterone synthesis and testicular health. Studies have shown that cyclophosphamide can lead to abnormal changes in these hormone levels, thereby affecting sperm production and maturation [35]. Therefore, in this study, a cyclophosphamide-induced asthenozoospermia mouse model was established and compared to the control group. Mice in the model group exhibited decreased testicular index, reduced sperm quality, and decreased serum FSH, LH, and T levels, along with evident pathological damage to testicular and epididymal tissues. Asthenozoospermia is currently primarily treated using hormones, antioxidants, etc [36]. However, owing to the uncertain efficacy and numerous side effects associated with some patients, acupuncture, as a characteristic diagnostic and therapeutic method for TCM, has gradually been applied in the treatment of asthenozoospermia. According to the TCM theory, kidney deficiency is the primary pathogenesis of asthenozoospermia, and the condition may also involve the spleen and stomach or be compounded by emotional factors [37]. The kidneys govern reproduction and serve as the foundation for innate vitality. Sperm production relies on the nourishment of the kidney. Sufficient kidney essence results in vigorous reproductive function and abundant sperm quantity and vitality. Conversely, insufficient kidney qi weakens reproductive essence, leading to reduced sperm quantity and quality. The spleen is considered to be the foundation of acquired vitality. If the kidneys lack nourishment for the acquired qi, it may affect the absorption of

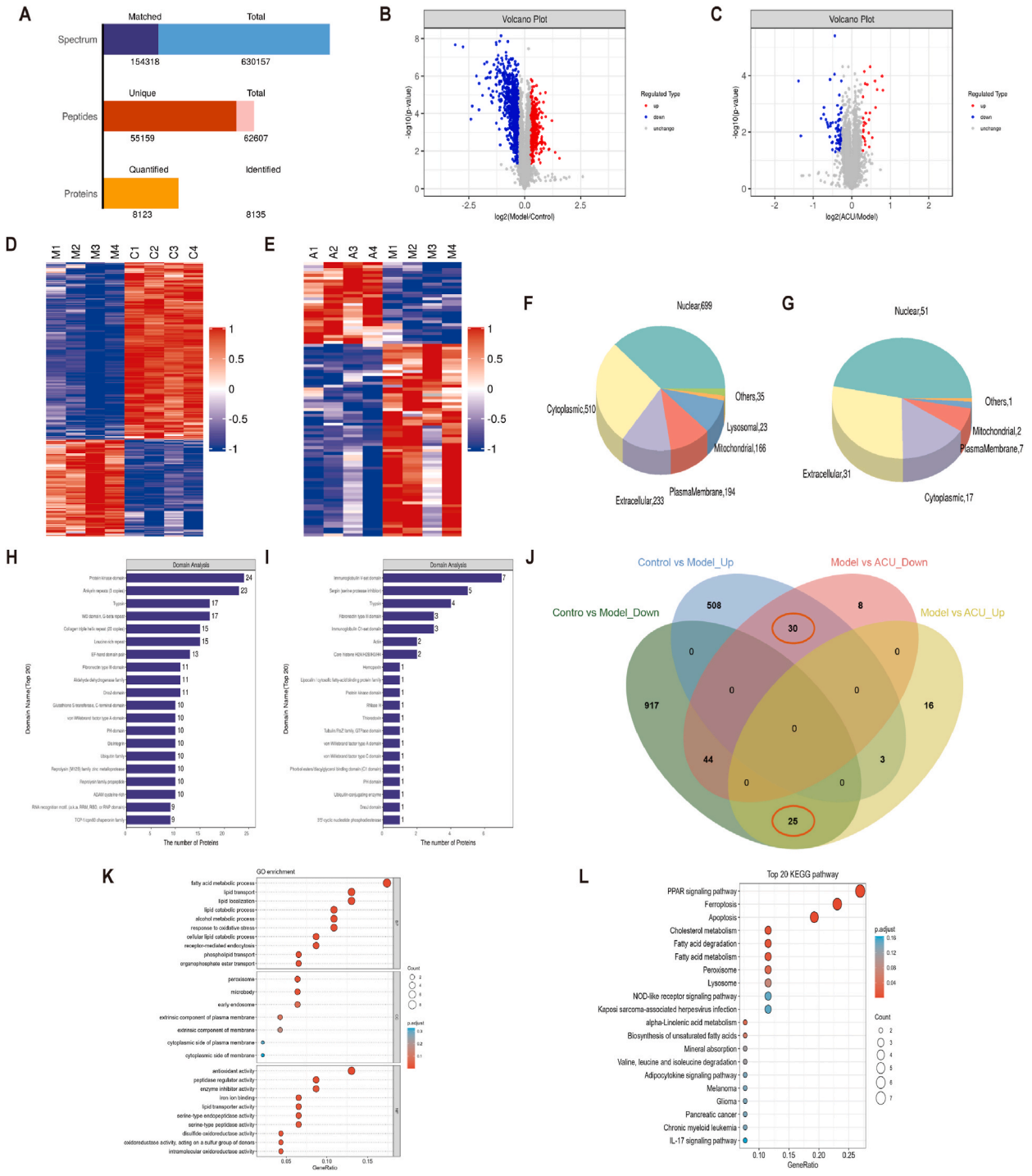

Fig. 3. Proteomic analysis. (A) Statistics of protein identification and quantification results. (B) Volcano plot of DEPs between control group vs. model group. (C) Volcano plot of DEPs between model group vs. ACU group. (D) Heatmap clustering of DEPs between control group vs. model group. (E) Heatmap clustering of DEPs between model group vs. ACU group. (F) Subcellular localization analysis of DEPs between control group vs. model group. (G) Subcellular localization analysis of DEPs between model group vs. ACU group. (H) Domain analysis of DEPs between control group vs. model group. (I) Domain analysis of DEPs between model group vs. ACU group. (J) Venn diagram of intersecting DEPs. (K) GO analysis. (L) KEGG analysis.

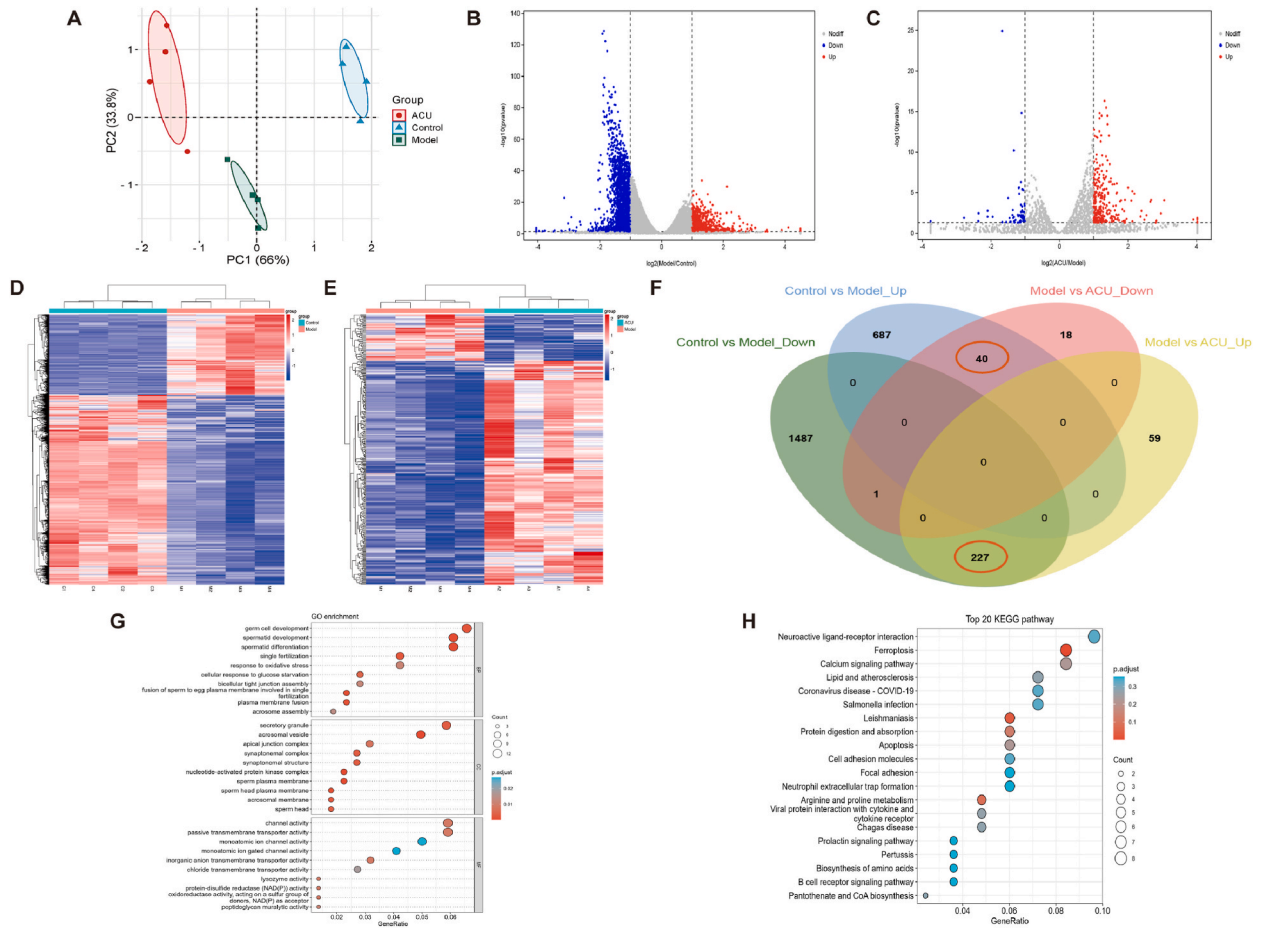

Fig. 4. Transcriptomic analysis. (A) Principal component analysis. (B) Volcano plot of DEGs between control group vs. model group. (C) Volcano plot of DEGs between model group vs. ACU group. (D) Heatmap clustering of DEGs between control group vs. model group. (E) Heatmap clustering of DEGs between model group vs. ACU group. (F) Venn diagram of intersecting DEGs. (G) GO analysis. (H) KEGG analysis.

nutrients and hinder sperm development and maturation. In addition, TCM emphasizes the impact of emotions on physical health. Prolonged mental stress, anxiety, depression, and other negative emotions may adversely affect the reproductive system. Therefore, the treatment of asthenozoospermia should focus on tonifying the spleen and kidneys, while also addressing psychological factors. In this study, we used the "Zhibian (BL 54)-to-Shuidao (ST 28)" acupuncture technique for intervention therapy. The Zhibian (BL 54)" is located in the sacrococcygeal region and is an acupuncture point of the Bladder Meridian of Foot-Taiyang. It is closely related to the Kidney Meridian, which activates the collaterals, regulates menstruation, and nourishes the kidneys. "Shuidao (ST 28)" is located in the lower abdomen and is an acupuncture point in the stomach meridian of foot yangming. It is closely related to the Spleen Meridian and regulates water pathways, tonifies the kidneys, and replenishes essence. By needling obliquely from "Zhibian (BL 54)-to-Shuidao (ST 28)," it can stimulate the pelvic plexus nerves and perineal nerves, allowing the meridian qi to reach the affected area, exerting a regulatory effect on reproductive organs such as the testes. In addition, patients may experience a sensation radiating to the perineum during acupuncture, which may have positive psychological effects. The "Zhibian (BL 54)-to-Shuidao (ST 28)" acupuncture technique is currently widely used in the treatment of various male and female reproductive system disorders [16–18]. This study found that after intervention with the "Zhibian (BL 54)-to-Shuidao (ST 28)" acupuncture technique, the testis and epididymis indices of mice improved, with varying degrees of improvement observed in testicular and epididymal pathological morphology. Furthermore, sperm quality improved, and serum FSH, LH, and T levels increased to varying degrees. These findings suggest that acupuncture enhances sperm motility in mice with asthenozoospermia by potentially correcting disorders in serum hormone levels and repairing damaged testicular and epididymal tissues, thereby effectively improving sperm vitality.

Apoptosis is a self-regulated mechanism of cell death that plays a crucial role in spermatogenesis and sperm development [38]. Throughout the process, from spermatogonia division to mature sperm formation, normal apoptosis enables the organism to eliminate abnormal or damaged sperm, thus finely regulating the quantity and quality of sperm and ensuring that the produced sperm possesses good quality and genetic information. However, excessive activation of apoptosis can lead to abnormal sperm morphology and functional impairments, affecting sperm motility and fertilization capacity within the reproductive system and consequently affecting the success rate of embryo development. Key proteins involved in the process of cell apoptosis include BCL-2, BAX, and Caspase-3 [39].

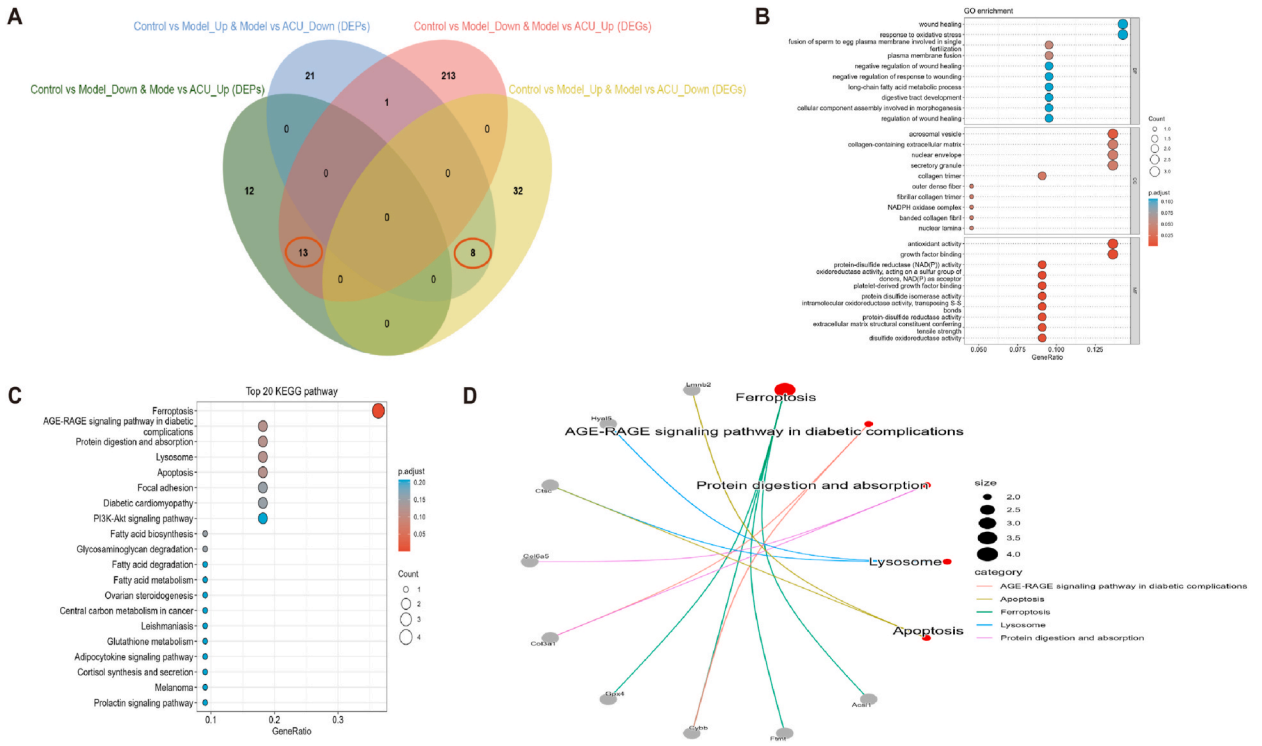

Fig. 5. Integrated transcriptomic and proteomic analysis. (A) Venn diagram showing the intersection of DEGs and DEPs. (B) GO analysis. (C) KEGG analysis. (D) KEGG enrichment cnet plot.

BCL-2 inhibits apoptosis by maintaining the integrity of mitochondrial membranes, whereas BAX induces apoptosis by increasing mitochondrial permeability; the balance between these two determines whether the cell survives or dies. Caspase-3, a key proteinase involved in apoptosis, triggers programmed cell death by cleaving and activating a series of intracellular proteins. Multiple studies have indicated that, compared to normal individuals, patients with asthenozoospermia or animals exhibit significantly elevated rates of sperm apoptosis and markedly decreased proliferation and migration abilities [40,41]. Our research findings showed that, compared to the control group, the model group exhibited increased germ cell apoptosis levels within the testicular tissue, along with varying degrees of elevation in BAX and Caspase-3 mRNA and protein expression levels, and a decrease in BCL-2 mRNA and protein expression levels, consistent with previous studies. Following acupuncture treatment, the level of germ cell apoptosis within the testicular tissue in the model group decreased, accompanied by varying degrees of reduction in BAX and Caspase-3 mRNA and protein expression levels, and an increase in BCL-2 mRNA and protein expression levels, suggesting that acupuncture may suppress abnormal apoptosis of germ cells within the testicular tissue by regulating key factors in the apoptosis pathway.

To further investigate the mechanisms underlying the improvement of asthenozoospermia by acupuncture, we conducted transcriptomic and proteomic analyses to examine the changes in RNA and protein levels in mouse testicular tissue. We focused on 55 DEPs and 267 DEGs that exhibited a reverse trend between the model group and the control group and the ACU group and the model group. Specifically, compared to the control group, 30 DEPs and 40 DEGs were upregulated in the model group and downregulated after acupuncture, whereas 25 and 227 DEGs were downregulated in the model group and upregulated after acupuncture. Subsequently, we conducted a functional enrichment analysis of 21 intersecting genes that were differentially expressed at both RNA and protein levels. Comprehensive analysis of GO and KEGG pathways indicated that the genes and proteins influenced by acupuncture in the context of asthenozoospermia primarily pertain to cellular components relevant to sperm structure and function. In addition, they are involved in processes associated with oxidative stress and antioxidant activity, notably through modulation of the ferroptosis signaling pathway. Ferroptosis is a novel iron-dependent form of programmed cell death that is distinct from apoptosis, necrosis, and autophagy. Research indicates that ferroptosis may be involved in spermatogenic cell division and differentiation, blood-testis barrier function, and testosterone secretion through pathways such as iron metabolism abnormalities, lipid peroxidation, oxidative stress, and mitochondrial damage, thereby affecting sperm development and maturation, and leading to male infertility such as asthenozoospermia [42–44]. Cellular iron accumulation is one of the typical markers of ferroptosis, as multiple studies have shown [45,46]. Iron metabolic disorders induced by an iron overload can lead to sperm defects and gonadal dysfunction, thereby affecting fertility. In this study, it was observed that after induction with cyclophosphamide, there was a significant increase in iron content in the testicular tissue, indicating the disruption of iron homeostasis in the testes of the model group mice. Excessive accumulation of iron ions can trigger cellular ferroptosis by generating reactive oxygen species through the Fenton reaction, which exacerbates lipid peroxidation. Physiological ROS levels play crucial roles in estrogen production, sperm energetics, cell signaling, acrosome reactions, and sperm motility.

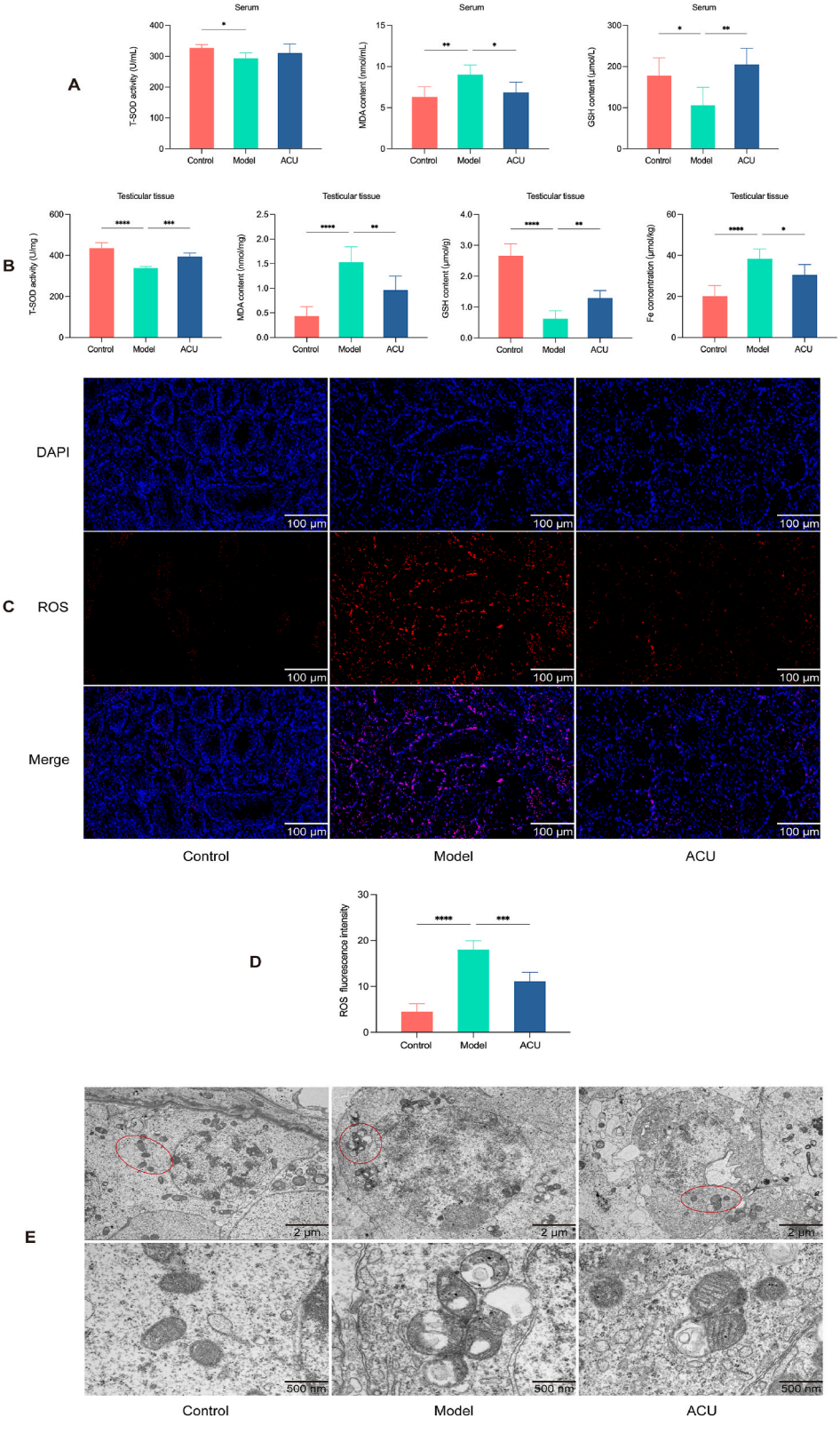

(caption on next page)

Fig. 6. Acupuncture improves oxidative stress and iron metabolism in asthenozoospermia mice. (A) Comparison of serum T-SOD activity, GSH, and MDA levels among groups. (B) Comparison of testicular tissue T-SOD activity, GSH, MDA, and total iron levels among groups. (C–D) Comparison of ROS levels in testicular tissue among groups. (E) Comparison of mitochondrial morphology in testicular tissue (× 4000, × 20000). Data are presented as mean ± SD. *$P < 0.05$; **$P < 0.01$, ***$P < 0.001$, ****$P < 0.0001$.

Studies have shown that increased ROS levels are a major cause of reduced sperm vitality [47–50]. Elevated ROS levels can damage the antioxidant systems of male sperm and seminal plasma, leading to damage to sperm structure and function through various pathways, such as attacking sperm membranes rich in unsaturated fatty acids, damaging sperm DNA single and double strands, and impairing mitochondria and mitochondrial DNA, thereby reducing sperm vitality. In addition, when ROS levels are excessive, they react with polyunsaturated fatty acids on the surface of sperm membranes, leading to the overproduction of MDA. At this point, the SOD content correspondingly decreases, weakening its ability to eliminate excess ROS in the body and resulting in a vicious cycle of elevated ROS levels in the body. Furthermore, excess ROS may disrupt the synthesis and reduction of GSH and other pathways, thereby disrupting the oxidative-reductive balance within sperm cells, triggering oxidative stress reactions, exacerbating ferroptosis, and ultimately reducing sperm vitality. This study indicates that acupuncture can significantly reduce ROS, MDA, and total iron levels and increase SOD and GSH levels in asthenozoospermic mice, thereby reducing oxidative stress reactions in sperm and improving sperm vitality. Typical morphological changes associated with ferroptosis include increased mitochondrial membrane density, reduced mitochondrial volume, and rupture or loss of cristae [51]. Mitochondria are powerhouses for cellular energy production and provide the energy required for sperm motility [52]. Proper mitochondrial function ensures an adequate supply of adenosine triphosphate (ATP), maintains a proper redox balance, and prevents ROS overproduction. However, abnormal mitochondrial morphology may disrupt mitochondrial DNA stability and structural integrity, leading to energy production impairment and affecting sperm motility and fertilization ability. This study found that acupuncture partially improved the morphology of damaged mitochondria.

This study found that ACSL1/CYBB/FTMT/GPX4, target genes of ferroptosis, may be closely related to improvements in reproductive function in asthenozoospermic mice following acupuncture. The ACSL family plays a crucial role in fatty acid synthesis and degradation by catalyzing the formation of acyl-coenzyme A from free fatty acids, thereby providing substrates for lipid metabolism pathways essential for ferroptosis [53]. Specifically, ACSL1 has been identified as a ferroptosis initiator capable of mediating linoleic acid synthesis from lipid peroxides, integrating them into neutral lipids, exacerbating membrane lipid peroxidation, and promoting cellular ferroptosis [54]. Furthermore, studies have shown that viral infection can upregulate ACSL1 expression and that the mediated ferroptosis process can induce inflammation and tissue damage [55]. NOX serves as the primary source of intracellular superoxide and plays a significant role in regulating cellular redox signaling and maintaining internal balance [56]. CYBB (also known as NOX2) is a member of the NOX family and primarily catalyzes the oxidase core. CYBB activation can lead to ROS accumulation and ferroptosis [57]. FTMT is an important mitochondrial iron storage protein with ferroxidase activity. Research has shown that FTMT catalyzes the conversion of ferrous iron to ferric iron for iron storage as well as regulates intracellular iron metabolism, inhibits the Fenton reaction, and reduces ROS production, thereby suppressing ferroptosis, which is crucial for maintaining cellular iron homeostasis and protecting mitochondria from oxidative stress damage [58,59]. GPX4 is widely expressed in normal mammalian tissues with relatively high expression levels in testicular tissues, especially in late-stage sperm cells [60]. Studies have shown that GPX4 participates in the condensation and decondensation of sperm chromatin, forming the sperm and mitochondrial sheaths. It can prevent testicular cell ferroptosis by clearing lipid peroxides and slowing the Fenton reaction [61–65]. Moreover, GPX4 deficiency-mediated cell ferroptosis may be associated with oxidative stress, inflammation, apoptosis, and autophagy crosslinking, affecting various stages of spermatogenesis and leading to male infertility. In this study, the ferroptosis-related indicators ACSL1/CYBB/FTMT/GPX4 were found to be primarily expressed in spermatocytes and mesenchymal cells. Compared with the control group, the model group showed elevated expression of ACSL1 and CYBB in the testicular tissue, whereas FTMT and GPX4 expression levels were decreased. After acupuncture, the expression of FTMT and GPX4 increased, whereas that of ACSL1 and CYBB decreased. These findings suggest that acupuncture has effects similar to those of ferroptosis inhibitors. It can enhance the antioxidant capacity of the testes by regulating the balance of ACSL1/CYBB/FTMT/GPX4, maintaining cellular iron homeostasis and preventing excessive ferroptosis of germ cells, thereby alleviating cyclophosphamide-induced testicular damage.

5. Conclusion

In summary, acupuncture can effectively regulate the disruption of serum hormone levels induced by cyclophosphamide in asthenozoospermic mice, repair damaged testicular and epididymal tissues, alleviate germ cell apoptosis, and improve reproductive functions. Its mechanism may involve lowering ACSL1 and CYBB expression in testicular tissue, increasing GPX4 and FTMT expression to alleviate ferroptosis, and consequently improving the oxidative stress status within cells. This study provides novel insights into acupuncture treatment for asthenozoospermia and presents positive implications for the application and promotion of the “Zhibian (BL 54)-to-Shuidao (ST 28)" acupuncture technique.

Data availability statement

The transcriptomic data have been deposited in the NCBI SRA database (https://www.ncbi.nlm.nih.gov/sra) with accession number PRJNA1133922. The proteomics data have been deposited in the ProteomeXchange Consortium database (https://www.ebi.ac.uk/pride) with accession number PXD053841.

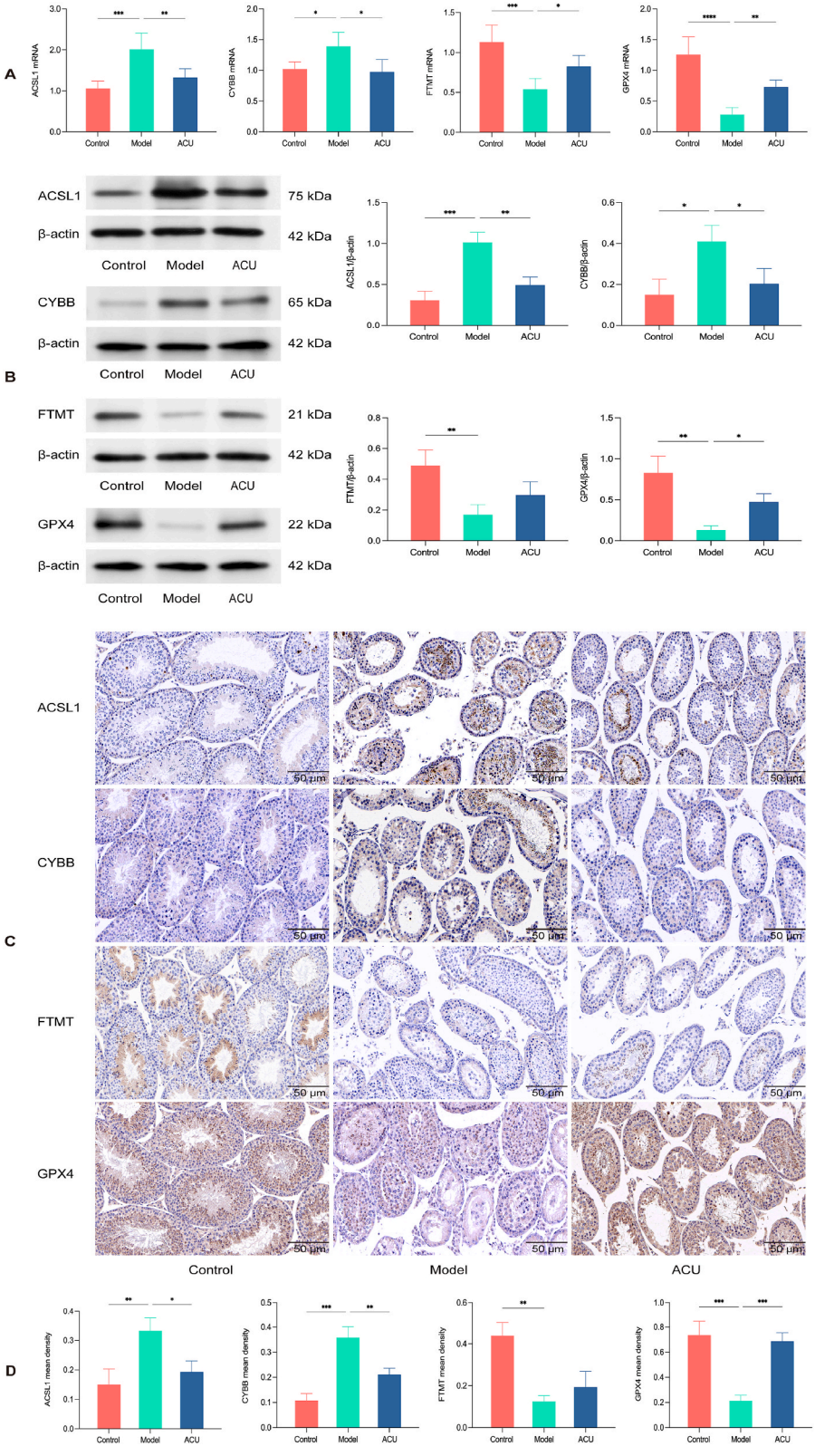

(caption on next page)

Fig. 7. Acupuncture improves testicular ferroptosis in asthenozoospermia mice by regulating ACSL1/CYBB/FTMT/GPX4. (A) Comparison of ACSL1/CYBB/FTMT/GPX4 mRNA expression levels in testicular tissue among groups (n = 5). (B) Comparison of ACSL1/CYBB/FTMT/GPX4 protein expression levels in testicular tissue among groups (n = 3) (Western blot original images are provided in Supplementary 3). (C–D) Comparison of ACSL1/CYBB/FTMT/GPX4 immunohistochemical in testicular tissue among groups (n = 3). Data are presented as mean ± SD. $^{*}P < 0.05$; $^{**}P < 0.01$, $^{***}P < 0.001$, $^{****}P < 0.0001$.

Ethics approval and consent to participate

The animal study were approved by the Experimental Animal Ethics Committee of Shanxi University of Traditional Chinese Medicine (approval No. AWE202303381).

Consent for publication

All authors consent to the publication of this work in Heliyon.

Funding

This work was funded by grants from National Natural Science of Foundation of China (82074549), Shanxi Provincial Administration of Traditional Chinese Medicine Foundation (2023ZYYB048).

CRediT authorship contribution statement

Jianheng Hao: Writing – review & editing, Writing – original draft, Software, Methodology, Investigation, Formal analysis, Data curation, Conceptualization. **Jia Ren:** Methodology, Formal analysis, Data curation. **Boya Chang:** Resources, Methodology, Investigation, Data curation. **Huichao Xu:** Resources, Methodology, Investigation, Data curation. **Haijun Wang:** Writing – review & editing, Supervision, Project administration. **Laixi Ji:** Writing – review & editing, Supervision, Project administration, Funding acquisition.

Declaration of competing interest

The authors declare that they have no known competing financial interests or personal relationships that could have appeared to influence the work reported in this paper.

Acknowledgements

We express our most sincere gratitude to all the professionals who selflessly participated in this study.

Appendix A. Supplementary data

Supplementary data to this article can be found online at https://doi.org/10.1016/j.heliyon.2024.e36664.

References

[1] A. Agarwal, S. Baskaran, N. Parekh, C.L. Henkel R. Vij S. Cho, M. Arafa, M.K. Panner Selvam, R. Shah, Male infertility, Lancet. 397 (2021) 319–333.
[2] World Health Organization, WHO Laboratory Manual for the Examination and Processing of Human Semen, fifth ed., World Health Organization, Geneva, 2021.
[3] S.Z. Shahrokhi, P.Alyasin A. Salehi, Taghiyar S. Deemeh, M.R. Asthenozoospermia, Cellular and molecular contributing factors and treatment strategies, Andrologia 52 (2020) e13463.
[4] C. Tu, W. Wang, T. Hu, G.Lin G. Lu, Y.Q. Tan, Genetic underpinnings of asthenozoospermia, Best Pract. Res. Clin. Endocrinol. Metabol. 34 (2020) 101472.
[5] L. Boeri, P. Capogrosso, E. Ventimiglia, F. Pederzoli, W. Cazzaniga, F. Chierigo, F. Dehò, E. Montanari, F. Montorsi, A. Salonia, Heavy cigarette smoking and alcohol consumption are associated with impaired sperm parameters in primary infertile men, Asian J. Androl. 21 (2019) 478.
[6] S.H. Zhou, Y.F. Deng, Z.W. Weng, H.W. Weng, Z.D. Liu, Traditional Chinese medicine as a remedy for male infertility: a review, World. J. Mens. Health 37 (2019) 175–185.
[7] J. Luo, Y. Luo, C. Dong, G. Qi, L. Liu F. Zhong, W. Wen, Enhancing sperm motility parameters in patients with asthenospermia: a combined approach of acupuncture at fusiguan point and tamoxifen citrate tablets, Arch. Esp. Urol. 77 (2024) 142–147.
[8] E.V. Kucuk, A. Bindayi, U. Boylu, F.F. Onol, E. Gumus, Randomised clinical trial of comparing effects of acupuncture and varicocelectomy on sperm parameters in infertile varicocele patients, Andrologia 48 (2016) 1080–1085.
[9] I. Nurwati, B. Murti, U.R. Budihastuti, T. Prakosa, A. Laqif, E. Melinawati, H. Prasetya, L. Susanto, M. Sukmawati, Electroacupuncture effectiveness for treating idiopathic male infertility, Med. Acupunct. 34 (2022) 405–409.
[10] J. Zhu, B. Arsovska, K. Kozovska, Acupuncture treatment for fertility, Open Access Maced J Med Sci 6 (2018) 1685–1687.
[11] H. Li Z. Huang, W. Liu J. Han, J.Mao J. Sun, P. Liu, Electroacupuncture regulates sperm motility in patients with asthenozoospermia: study protocol for a randomized sham-controlled clinical trial, Minerva Med. 114 (2023) 906–909.
[12] Yu Y. Sha S.B. Zhang B. Guan, Q. Liang M. Zhao, L.G. Zhang, Q.Y. Wen J, W. Sun, Effects and mechanism of action of transcutaneous electrical acupuncture point stimulation in patients with abnormal semen parameters, Acupunct. Med. 37 (2019) 25–32.

[13] J. Gao, Y. Zuo, K.H. So, W.S. Yeung, E.H. Ng, K.F. Lee, Electroacupuncture enhances spermatogenesis in rats after scrotal heat treatment, Spermatogenesis 2 (2012) 53–62.
[14] T. Cui, W. Qin, M. Liu, B.X. Gao, Y.X. Ma, X.P. Zhang, Effect of electroacupuncture on spermatogenesis in rats with oligozoospermia of insufficiency of shen (kidney) essence syndrome, Chin. J. Integr. Med. 25 (2019) 292–297.
[15] Z.R. Jin, B.H. Liu, J. Cai, X.H. Jing, B. Zhu, G.G. Xing, Experimental study on electroacupuncture for asthenozoospermia in rats, Acupunct. Res. 42 (2017) 114–118.
[16] J. Yan, M.N. Ma, J.Y. Zhao, H.Y. Wang, L.Y. Yin, Effect of "Zhibian" (BL 54)-to-"Shuidao" (ST 28) needle insertion on the expression of Fas/FADD/Caspase-8 of death receptor pathway in rats with primary ovarian insufficiency, Chin. Acupunct. Moxibustion 43 (2023) 537–544.
[17] C.Y. Hao, T.S. Zhang, J.M. Qi, L.X. Ji, Observation on the therapeutic effect of " Zhibian"(BL 54)-to-"Shuidao" (ST 28) on polycystic ovary syndrome, Chin. Acupunct. Moxibustion 35 (2015) 461–464.
[18] H.J. Wang, Cao Y.X. Ji J.Q. Xu N.H. Ji L.X. Clinical observation on the treatment of primary dysmenorrhea patients with the "Zhibian" (BL 54)-to-"Shuidao" (ST 28) acupuncture method, Chin. J. Integr. Tradit. West. Med. 39 (2019) 1266–1268.
[19] H. Zhang, L. He, Cai L. Transcriptome sequencing: RNA-seq, Comp Syst Biol 1754 (2018) 15–27.
[20] B.T. Ruotolo, Collision cross sections for native proteomics: challenges and opportunities, J. Proteome Res. 21 (2021) 2–8.
[21] N. Li, X. Dong, S. Fu, X. Wang, H. Li, G. Song, D. Huang, C-type natriuretic peptide (cnp) could improve sperm motility and reproductive function of asthenozoospermia, Int. J. Mol. Sci. 23 (2022) 10370.
[22] J.H. Hao, J. Ren, B.Y. Chang, H.J. Wang, L.X. Ji, Effect of"Zhibian (BL 54)-to-Shuidao (ST 28)" acupuncture stimulation on key factors of apoptotic pathways inside and outside the testes in mice with asthenozoospermia, J. Tradit. Chin. Med. 65 (2024) 86–93.
[23] D. Tang, G. Kroemer, Ferroptosis, Curr. Biol. 30 (2020) 1292–1297.
[24] S. Cong, J. Zhang, F. Pan L. Zhang A. Ma J. Pan, Research progress on ion channels and their molecular regulatory mechanisms in the human sperm flagellum, Faseb. J. 37 (2023) e23052.
[25] M. Ahlmann, G. Hempel, The effect of cyclophosphamide on the immune system: implications for clinical cancer therapy, Cancer Chemother. Pharmacol. 78 (2016) 661–671.
[26] X. Liu, Q. Li, Z. Wang, F. Liu, Identification of abnormal protein expressions associated with mouse spermatogenesis induced by cyclophosphamide, J. Cell Mol. Med. 25 (2021) 1624–1632.
[27] S.J. Tsai, L.H. Li, W.J. Chen, E.Y. Huang, C.Y. Huang, R.E. Brannigan, W.J. Huang, I.S. Huang, Prediction of microdissection testicular sperm extraction outcomes of azoospermic patients post-chemotherapy using cyclophosphamide equivalent dose, J. Assist. Reprod. Genet. 40 (2023) 2013–2020.
[28] J.V. Medrano, D. Hervás, T. Vilanova-Pérez, A. Navarro-Gomezlechon, E. Goossens, A. Pellicer, M.M. Andrés, E. Novella-Maestre, Histologic analysis of testes from prepubertal patients treated with chemotherapy associates impaired germ cell counts with cumulative doses of cyclophosphamide, ifosfamide, cytarabine, and asparaginase, Reprod. Sci. 28 (2021) 603–613.
[29] M.K. Demirören S. Üçöz M. Oztatlici M. Özbilgin, Cyclophosphamide suppresses spermatogenesis in the testis of mice through downregulation of miR-34b and miR-34c, Andrologia 53 (2021) e14071.
[30] E. Ghobadi, M. Moloudizargari, M.H. Asghari, M. Abdollahi, The mechanisms of cyclophosphamide-induced testicular toxicity and the protective agents, Expert. Opin. Drug. Metab. 13 (2017) 525–536.
[31] D.J. Handelsman, Testosterone, spermatogenesis, and unravelling the mysteries of puberty, Endocrinology 161 (2020) 120.
[32] D. Santi, P. Crépieux, E. Reiter, G. Spaggiari, G. Brigante, L. Casarini, V. Rochira, M. Simoni, Follicle-stimulating hormone (FSH) action on spermatogenesis: a focus on physiological and therapeutic roles, J. Clin. Med. 9 (2020) 1014.
[33] A.S. López-Torres, M. Chirinos, Modulation of human sperm capacitation by progesterone, estradiol, and luteinizing hormone, Reprod. Sci. 24 (2017) 193–201.
[34] S. Ramaswamy, G.F. Weinbauer, Endocrine control of spermatogenesis: role of FSH and LH/testosterone, Spermatogenesis 4 (2014) e996025.
[35] S. Saleh, A. Ghanaatpisheh, H. Parvin N. Haghshenas, E. Kargar Jahromi H. Ebrahimi B. Mikaeiliagah, The effect of leaf hydroalcoholic extract of Ephedra pachyclada infertility in male rats treated with cyclophosphamide: an experimental study, Int. J. Reprod. Biomed. 21 (2023) 285.
[36] S.Z. Shahrokhi, P.Alyasin A. Salehi, Taghiyar S. Deemeh, M.R. Asthenozoospermia, Cellular and molecular contributing factors and treatment strategies, Andrologia 52 (2020) e13463.
[37] X.Y. Jiang, S.H. Chen, J.G. Cao, Discussion on treatment of asthenospermia from the perspective of psychosomatic medicine of traditional Chinese medicine, Psychosom. Med. Res. 3 (2021) 122–128.
[38] A. Asadi, R. Ghahremani, A. Abdolmaleki, F. Rajaei, Role of sperm apoptosis and oxidative stress in male infertility: a narrative review, Int. J. Reprod. Biomed. 19 (2021) 493–504.
[39] V. Changizi, O. Azadbakht, R. Ghanavati, H. Behrouj, E. Motevaseli, P. Khanzadeh, Effect of Lactobacillus species on apoptosis-related genes BCL2, BAX, and caspase 3 in the testes of gamma-irradiated rats, Rev. Assoc. Med. Bras. 67 (2021) 1581–1585.
[40] G. Li, P. Zhang, Y. You, D. Chen, J. Cai, Z. Ma, X. Huang, D. Chang, Qiangjing tablets regulate apoptosis and oxidative stress via Keap/Nrf2 pathway to improve the reproductive function in asthenospermia rats, Front. Pharmacol. 12 (2021) 714892.
[41] F. Li, A. Niu, K. Zhao, J. Feng, Y. Chen, GRIM-19 in asthenozoospermia regulates GC-2 spd cell proliferation, apoptosis and migration, Sci. Rep. 13 (2023) 3106.
[42] X. Yang, Y. Chen, W. Song, T. Huang, Y. Wang, Z. Chen, F. Chen, Y. Liu, X. Wang, C. Zhang, Review of the role of ferroptosis in testicular function, Nutrients 14 (2022) 5268.
[43] W. Yuan, Z. Sun, H. Hu, Emerging roles of ferroptosis in male reproductive diseases, Cell Death Dis. 9 (2023) 358.
[44] Y. Su, Z. Liu, K. Xie, Y. Li C. Ren, W. Chen, Ferroptosis: a novel type of cell death in male reproduction, Genes 14 (2022) 43.
[45] J. Wang, Z. Zhang, F. Shi, Y. Li, Y. Tang, C. Liu, Y. Wang, J. Chen, X. Jiang, H. Yang, L. Sun, Q. Chen, L. Ao, J. Cao, PM2. 5 caused ferroptosis in spermatocyte via overloading iron and disrupting redox homeostasis, Sci. Total Environ. 872 (2023) 162089.
[46] Y. Wang, J. Wu, M. Zhang, H. OuYang, M. Li, D. Jia, R. Wang, W. Zhou, H. Hu Y. Liu, Y. Liu Y. Yao, Y. Ji, Cadmium exposure during puberty damages testicular development and spermatogenesis via ferroptosis caused by intracellular iron overload and oxidative stress in mice, Environ. Pollut. 325 (2023) 121434.
[47] K. Nowicka-Bauer, B. Nixon, Molecular changes induced by oxidative stress that impair human sperm motility, Antioxidants 9 (2020) 134.
[48] P. Zhang S. Meng, X. Jiang, S. Cheng, J. Zhang, X. Cao, X. Qin, Z. Zou, C. Chen, Arsenite induces testicular oxidative stress in vivo and in vitro leading to ferroptosis, Ecotoxicol. Environ. Saf. 194 (2020) 110360.
[49] H. Zhu, Y. Cheng, X. Wang, X. Yang, M. Liu, J. Liu, S. Liu, H. Wang, A. Zhang, R. Li, C. Ye, J. Zhang, J. Gao, X. Fu, B. Wu, Gss deficiency causes age-related fertility impairment via ROS-triggered ferroptosis in the testes of mice, Cell Death Dis. 14 (2023) 845.
[50] L. Li, M.Y. Wang, H.B. Jiang, C.R. Guo, X.D. Zhu, X.Q. Yao, W.W. Zeng, Y. Zhao, L.K. Chi, Bisphenol A induces testicular oxidative stress in mice leading to ferroptosis, Asian J. Androl. 25 (2023) 375.
[51] H. Wang, C. Liu, Y. Zhao, G. Gao, Mitochondria regulation in ferroptosis, Eur. J. Cell Biol. 99 (2020) 151058.
[52] F. Barbagallo, S. La Vignera, R. Cannarella, A. Aversa, A.E. Calogero, R.A. Condorelli, Evaluation of sperm mitochondrial function: a key organelle for sperm motility, J. Clin. Med. 9 (2020) 363.
[53] J.Y. Lee, W.K. Kim, K.H. Bae, S.C. Lee, E.W. Lee, Lipid metabolism and ferroptosis, Biology 10 (2021) 184.
[54] A. Beatty, T. Singh, Y.Y. Tyurina, V.A. Tyurin, S. Samovich, E. Nicolas, K. Maslar, Y. Zhou, K.Q. Cai, Y. Tan, S. Doll, M. Conrad, A. Subramanian, H. Bayır, V. E. Kagan, U. Rennefahrt, J.R. Peterson, Ferroptotic cell death triggered by conjugated linolenic acids is mediated by ACSL1, Nat. Commun. 12 (2021) 2244.
[55] H. Xia, Z. You F. Zhang, Inhibiting ACSL1-related ferroptosis restrains murine coronavirus infection, Viruses 13 (12) (2021) 2383.
[56] F. Kuang, J. Liu, D. Tang, R. Kang, Oxidative damage and antioxidant defense in ferroptosis, Front. Cell Dev. Biol. 8 (2020) 586578.
[57] I.C. Su, Y.K. Su, S.A. Setiawan, V.K. Yadav, I.H. Fong, C.T. Yeh, C.M. Lin, H.W. Liu, Nadph oxidase subunit cybb confers chemotherapy and ferroptosis resistance in mesenchymal glioblastoma via nrf2/sod2 modulation, Int. J. Mol. Sci. 24 (2023) 7706.
[58] Y.Q. Wang, S.Y. Chang, Q. Wu, Y.J. Gou, L. Jia, Y.M. Cui, P. Yu, Z.H. Shi, W.S. Wu, G. Gao, Y.Z. Chang, The protective role of mitochondrial ferritin on erastin-induced ferroptosis, Front. Aging Neurosci. 8 (2016) 308.

[59] S. Levi, M. Ripamonti, M. Dardi, A. Cozzi, P. Santambrogio, Mitochondrial ferritin: its role in physiological and pathological conditions, Cells 10 (2021) 1969.
[60] R. Brigelius-Flohé, L. Flohé, Regulatory phenomena in the glutathione peroxidase superfamily, Antioxidants Redox Signal. 33 (2020) 498–516.
[61] P. Liu, J. Zhu, G. Li D. Yuan, Y. Wen, S. Huang, Z. Lv, Y. Guo, J. Cheng, The effects of selenium on GPX4-mediated lipid peroxidation and apoptosis in germ cells, J. Appl. Toxicol. 42 (2022) 1016–1028.
[62] Y. Xie, R. Kang, D.J. Klionsky, D. Tang, GPX4 in cell death, autophagy, and disease, Autophagy 19 (2023) 2621–2638.
[63] X. Hao, H. Wang, F. Cui, Z. Yang, L. Ye, R. Huang, J. Meng, Reduction of SLC7A11 and GPX4 contributing to ferroptosis in sperm from asthenozoospermia individuals, Reprod. Sci. 30 (2023) 247–257.
[64] J. Ding, B. Lu, L. Liu, Z. Zhong, N. Wang, B.Sheng W. Li, Q. He, Guilu-Erxian-Glue alleviates Tripterygium wilfordii polyglycoside-induced oligoasthenospermia in rats by resisting ferroptosis via the Keap1/Nrf2/GPX4 signaling pathway, Pharm. Biol. 61 (2023) 213–227.
[65] R. Zhuge, Z. Li, C. He, W. Ma, J. Yan, Q. Xue, R. Wang, Y. Liu, R. Lu, H. Du, F. Yin, L. Guo, Bone marrow mesenchymal stem cells repair hexavalent chromium-induced testicular injury by regulating autophagy and ferroptosis mediated by the AKT/mTOR pathway in rats, Environ. Toxicol. 38 (2023) 289–299.